Robust deep learning framework for the detection of melanoma in images

Trisha Sarkar
Dept. of Computer Engineering
MPSTME, NMIMS University
Mumbai, India
trisha9sarkar@gmail.com

Anushka Khare
Dept. of Computer Engineering
MPSTME, NMIMS University
Mumbai, India
anushkakhare0202@gmail.com

Mohit Parekh
Dept. of Computer Engineering
MPSTME, NMIMS University
Mumbai, India
mohitparekh19@gmail.com

Param Mehta
Dept. of Computer Engineering
MPSTME, NMIMS University
Mumbai, India
parammehta2000@gmail.com

Avani Bhuva
Assistant Professor,
MPSTME, NMIMS University
Mumbai, India
avani.shah@nmims.edu

***Abstract*- Melanoma, a type of skin cancer, occurs when melanocytes become cancerous and is a common cause of death in adults. The presence of melanoma can be conclusively proved through biopsies, but these lap reports often take time. Early detection of melanoma could improve mortality rates and reduce costs. AI-based assistive tools can aid early detection. Most studies focus on detection either in dermoscopic images or in non-dermoscopic images, not both. In this paper, we propose a novel generalised framework which can detect melanoma in both dermoscopic and non-dermoscopic images. The framework includes a preprocessing pipeline, data augmentation and resolving class imbalances, followed by a VGG-16 model. The model gives a sensitivity (for melanoma cases) of 87% on non-dermoscopic images and 91% on dermoscopic images.**

***Keywords*- Melanoma, Transfer learning, VGG-16, Classification, Dermoscopic images, Clinical images**

I. INTRODUCTION

Cancer is a broad word for a variety of diseases in which normal cells transform into tumour cells in a multi-stage process. It is one of the top causes of mortality globally, that accounts for nearly 10 million deaths in the year 2020, or nearly one in six deaths [1]. Melanoma is a type of skin cancer that develops when the pigment-producing cells in the skin, called melanocytes, become malignant. Melanoma is most usually caused by UV skin damage. It is the fifth most common form of cancer in adults and the deadliest form of skin cancer. The Caucasian populations are at a higher risk of melanoma skin cancer because of their relative lack of skin pigmentation [2]. In the year 2020, there were approximately 9,958,133 deaths worldwide due to cancer, out of which 57,043 deaths were due to melanoma of the skin [3],[4].

Early detection of melanoma is more beneficial than late-stage treatment as it reduces chances of long-term adverse effects, lower overall care costs and even saves the lives of patients who may not have responded to treatments. From the different types of cancer, it can be said that melanoma is easier to detect as it occurs on visible parts of the skin [5]. The stage of melanoma can be identified by biopsy or excising the suspected lesion and it is important to identify it for further prognosis and treatment [6]. Melanoma might be difficult to identify due its complexities but several criteria are available to help identify a cancerous lesion. The ABCDE criterion, which stands for Asymmetry, Border irregularity, Color textures, Diameter, and Evolution of a mole, includes the most prominent features but some moles can have several or all of the mentioned properties [7]. The Seven Point Checklist consists of seven parameters that take into account both chromatic aspects as well as those relating to the lesion's shape and structure [8]. The decision of whether a biopsy is required or not can also be taken using differential recognition (Ugly Duckling sign), pattern recognition (Beauty and the Beast sign), analytical recognition (Little Red Riding Hood sign), and comparative recognition [9]. The following features can also be used to help identify if the lesion is of melanoma: pigment networks, streaks, dots and globules, regression structures, blue-whitish veil, etc [10].

Melanoma can be identified via dermoscopic images obtained from dermoscopes, a specialized equipment that makes the inspection process easier by enlarging the lesion and providing uniform illumination. But, they are not as accessible as non-dermoscopic images tend to be. These photographs are usually obtained by ordinary cameras and result in what can be seen with the naked eye. This can be used to assess the danger of suspicious skin lesions prior to surgery, as well as to prioritize screening and appointment scheduling for patients. Though, they may have variations in illumination, less detailed information, and poorer contrast [11]. Both dermoscopic and non-dermoscopic images have advantages for diagnosis; for example, dermoscopic images depict better details, whilst non-dermoscopic images are widely available and can be used in clinical support systems to facilitate early and affordable diagnosis. This paper introducces a novel robust deep learning-based pipeline which can detect melanoma in non-dermoscopic as well as dermoscopic images. The model was trained and tested on sets including both kinds of images. The model has an overall sensitivity of 89% for melanoma.

The research paper has been organized into sections as follows: Section II expands on the literature review; Section III explains the methodology followed; Section IV discusses the results obtained; Section V presents the conclusions, and Section VI mentions the references.

II. LITERATURE SURVEY

Substantial research has been conducted to detect melanoma and even its size using various deep learning and computer vision techniques. Various criteria have also been used for the same. Dermoscopic images have been extensively used for melanoma prediction in various studies while studies

978-1-6654-9291-1/22/$31.00 ©2022 IEEE.

exploring non-dermoscopic images are limited as they contain less detailed information. To help identify melanoma in clinical images, a study proposed ten features based on different color characteristics of melanoma [12].

Machine learning techniques like SVM have been used to predict melanoma on the basis of asymmetry [13] or based on colour, texture or both [14] in dermoscopic images whereas, for non dermoscopic, SVM was used after illumination correction and region extraction, which gave an accuracy of 74.89% [15]. Naive Bayes has also been used for classifying malignant or benign melanoma lesions in dermoscopic images based on ABCD features, which gave an accuracy of 78% [7]. Fast Discriminative Mixed Membership based Naive Bayesian (FDMMNB) classifier was used for classification in non-dermoscopic images with 55.83% accuracy. Neural networks and random forests were also employed for prediction in non dermoscopic images, which gave accuracies of 67% and 76.28% respectively [15]. An artificial neural network ensemble method, which consisted of ANNs of varying network structures and fuzzy neural networks, was also used for melanoma classification in dermoscopic images [16].

Deep learning techniques like Convolutional Neural Networks (CNN) have been utilized for the prediction of melanoma for both dermoscopic and non-dermoscopic images [17] It has also been employed for the segmentation of melanoma lesions from dermoscopic images [18]-[21] and even from non-dermoscopic images [22],[23], after which it was also used for prediction. Pre-trained CNN models have also been employed using transfer learning techniques made available by the Keras library. The models most employed for melanoma detection in dermoscopic images were VGG-16 [24] and AlexNet [25]. A comparative study between different deep learning approaches for melanoma prediction was done by researchers, which concluded that ResNet50 along with data augmentation gave the best results [26]. Studies are also being held to integrate melanoma detection models with mobile applications to make the detection of melanoma more accessible and to be able to use images taken through smartphones for the same [27],[28].

Table I. Summary of the literature review conducted

Literature reference	Image type	Dataset Used	Model used	Accuracy obtained
[13]	Dermoscopic only	DermQuest	SVM	80%
[14]	Dermoscopic only	PH^2	SVM	96%
[15]	Non-Dermoscopic only	DermNet	SVM	74.89%
			ANN	67%
			FDMMNB	55.83%
			Random forest	76.28%
[7]	Dermoscopic only	PH^2	Naive Bayes	78%
[16]	Dermoscopic only	Images supplied by General Hospital of the Air Force of the Chinese Peoples Liberation Army	ANN Ensemble	94.17%
[17]	Non-Dermoscopic only	MED-NODE	CNN	81%

Based on our survey, the studies also utilize a combination of datasets for their research like MED-NODE [29] and DermNet [30] for non dermoscopic images while PH^2 [31] and HAM10000 [32] for dermoscopic images.

There seems to be scope to explore using a generalized model for predicting melanoma in both dermoscopic and non dermoscopic images. Our research aims to explore using a generalized transfer learning model for the prediction of melanoma in both dermoscopic and non dermoscopic images.

III. METHODOLOGY

In this study, the flow of steps that have been followed is shown in Figure 1. Each step has been explained in further detail in the subsequent subsections.

A. Dataset:

Two kinds of datasets have been used for the purpose of this study - a dataset of dermoscopic images and another dataset of non-dermoscopic images. These datasets were used for this study as they are popularly used for

melanoma use cases and are open-source datasets. The datasets used are as follows:

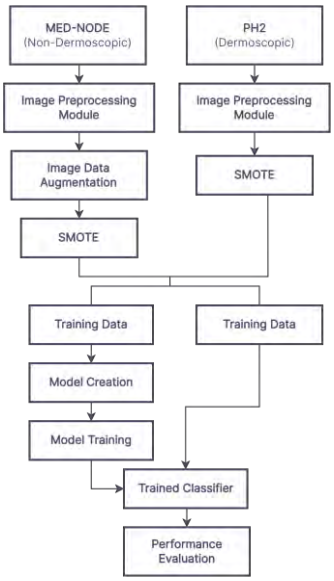

Fig. 1 Process for training and testing

- PH^2 [31] dataset consists of dermoscopic images, which have been captured dermatologically using a dermoscope. The dataset includes images of size 768x560 and a .csv file containing information about the diagnosis and various features present in each image. The images are categorised into three classes - common nevi (80 images), atypical nevi (80 images), and melanomas (40 images). Since a binary classification relating to the existence of melanoma is needed, we re-categorised the data into 2 classes - melanoma (40 images) and non-melanoma (160 images), by combining the other 2 classes.

- MED-NODE [29] dataset consists of non-dermoscopic images, taken using normal cameras with microlens. It contains images of size belonging to 2 categories - melanoma (70 images) and nevus images (100 images)

B. *Pre-processing*

To improve the model's ability to predict melanoma, both dermoscopic and non dermoscopic images were pre-processed using the same methods. The images were first processed to remove hair from them using image processing techniques to get a clear view of the lesion. The images were converted to grayscale and Black Hat transform was performed on them using a plus-shaped structuring element of size 17 x 17 pixels. Black Hat transform is essentially the difference between the image after the morphological closing operation and the original image. Then, the hair contours were intensified using binary thresholding with a threshold of 10 and a mask was generated. Inpainting was performed using the inpaint_telea method on the original image using the mask generated by binary thresholding. Inpainting in images is the process of filling in missing data in a specific region in the original image. The images were then resized to 224 x 224 pixels, so they confer to the required input size for the VGG-16 model and the pre-processing function provided by Keras was VGG-16 was used on the resized images to make them suitable for use as input on the transfer learning model.

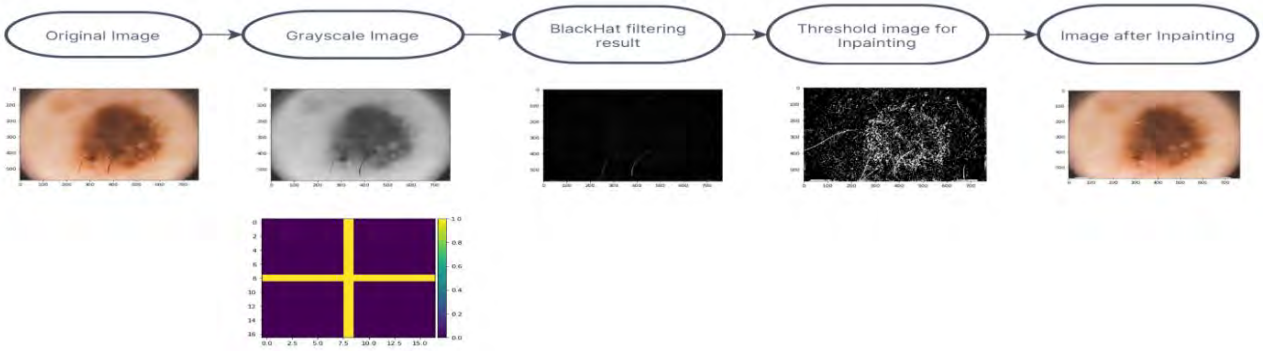

Fig. 2 Hair Removal process

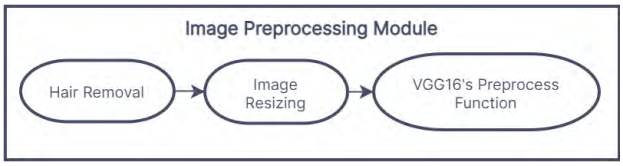

Fig. 3 Image Preprocessing Module

C. *VGG16 Model*

The transfer learning model VGG-16 was used as the Convolutional Neural Network model for melanoma prediction. VGG-16 is a deep neural network model with 16 layers and an extensive network that was trained on ImageNet dataset [33] images and the pre-trained model provided for use by the Keras library. The architecture of VGG-16 was retained, except for the output layer, and Dropout and Dense layers were added to the model. The activation function for the output layer was the Sigmoid function, as it is a classification problem. For the same reason, the loss function was binary cross entropy and the optimizer chosen was Stochastic Gradient Descent with Momentum. The learning rate for the optimizer was set to 0.001 and momentum was set to 0.85. Gradient clipping was done to avoid the problem of gradient explosion by utilising the clipnorm attribute for SGD. The metrics used for performance evaluation were accuracy and loss.

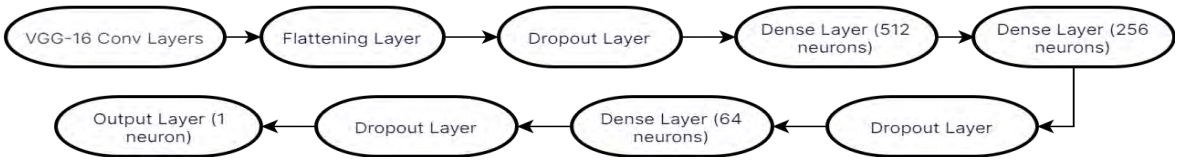

Fig. 4 Model architecture

Before training, data augmentation was applied with various parameters like rotation, slipping, shearing, flipping, etc. to increase the number and type of images in the non-dermoscopic dataset. Then, Synthetic Minority Oversampling Technique (SMOTE) was employed to address the class imbalance between melanoma and non-melanoma images in both dermoscopic and non-dermoscopic datasets, since the melanoma images are a minority class and that impacts the sensitivity of the model. The labels of the dataset were also changed to only have two labels to ensure the model predicts if the lesion is melanoma or nevus only. The model was trained and tested on both non-dermoscopic images and dermoscopic images, after splitting them into training and testing sets using stratify such that the ratio of images for both classes in the training and testing sets remains the same as that in the original dataset.

IV. RESULTS AND DISCUSSION

A. *Overall Model evaluation*

Class label 0 (negative) indicates non-melanoma and class label 1 (positive) indicates melanoma. The training and validation accuracy curves are increasing, as seen in Fig. 5. Fig 6 shows the steady decrease in the loss values across the epochs, indicating a steady optimisation by the SGD optimiser. The false negatives (undetected melanoma cases) are low, giving rise to a sensitivity of 89% for the overall model. From Fig, 7 it can be seen that the number of true positives and true negatives is higher as compared to the false positives and false negatives, indicating the correct classification of melanoma and non-melanoma overall. The training accuracy at the final epoch is seen to be 79.77% and the validation accuracy is 79%, which has been demystified further as we evaluate the performance on the specific type of image.

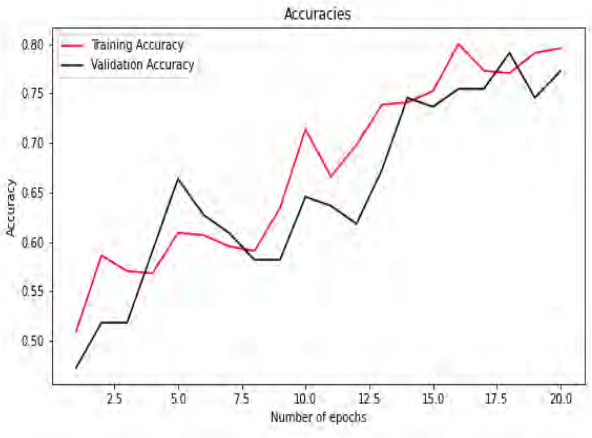

Fig. 5 Accuracy Curves

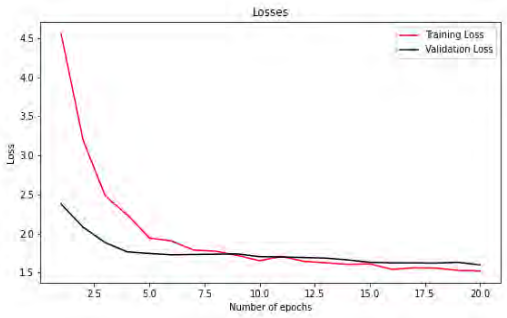

Fig. 6 Loss Curves

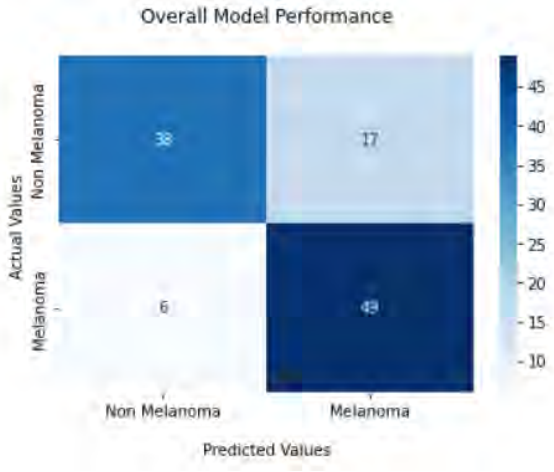

Fig. 7 Confusion matrix for overall model

B. *Model Evaluation on Non-Dermoscopic Images*

Based on Fig 8 and Fig 9, the following significant observations can be made about the model performance when tested on non-dermoscopic images. The non-melanoma class records a higher precision than the melanoma, indicating that of all the lesions labelled as non-melanoma, a higher number of lesions were indeed non-melanoma; compared to that of melanoma. A more important statistic is recall, especially for the target class. The melanoma class has a recall of 87% indicating that 87% of actual melanoma cases were correctly identified. Accuracy is a measure of correctness and simply computes the number of correct predictions against the number of total predictions, which was found to be 63%. The f1-score is higher for the class melanoma at 70%, which indicates that the model is good at correctly classifying melanoma as compared to non-melanoma in non-dermoscopic images. The key point to note is that the false negative cases, i.e., cases of actual melanoma cases that we predicted as non-melanoma, are lower than the false positive cases, i.e., cases of non-melanoma predicted as melanoma. This is

of importance since the criticality of diagnosis lies in the identification of the target class (melanoma) as much as possible.

	precision	recall	f1-score	support
Non-melanoma	0.75	0.39	0.51	23
Melanoma	0.59	0.87	0.70	23
accuracy			0.63	46
macro avg	0.67	0.63	0.61	46
weighted avg	0.67	0.63	0.61	46

Fig. 8 Classification report for non-dermoscopic images

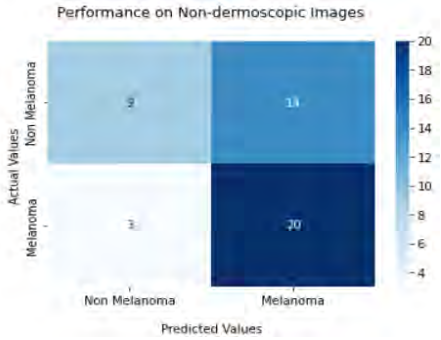

Fig. 9 Confusion matrix for non-dermoscopic images

C. *Model Evaluation on Dermoscopic Images*

Based on Fig 10 and Fig 11, the following significant observations can be made about the model performance when tested on dermoscopic images. The non-melanoma class records a higher precision than the melanoma for dermoscopic images as well. The melanoma class has a recall of 91% indicating that 91% of actual melanoma cases were correctly identified. The accuracy of the model, when tested on dermoscopic images, was found to be 77%. The f1-score is almost similar for both classes, which indicates that the model is equally good at correctly classifying melanoma well as non-melanoma in dermoscopic images. The number of false negatives is more than the number of false positives for dermoscopic images as well.

	precision	recall	f1-score	support
Non-melanoma	0.87	0.62	0.73	32
Melanoma	0.71	0.91	0.79	32
accuracy			0.77	64
macro avg	0.79	0.77	0.76	64
weighted avg	0.79	0.77	0.76	64

Fig. 10. Classification report for dermoscopic images

V. CONCLUSION

This paper suggests a robust deep-learning approach for the detection of melanoma in dermoscopic and non-dermoscopic images. The dermoscopic and non-dermoscopic images are pre-processed using an inpainting-based hair removal technique and VGG16's pre-processing module.

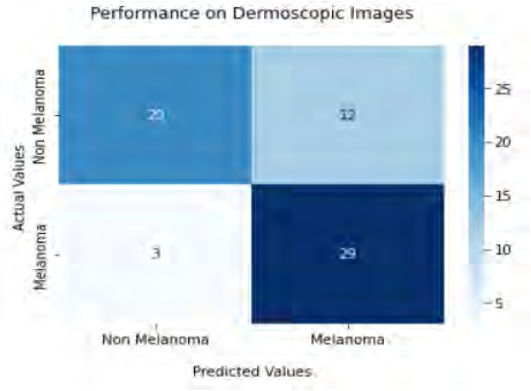

Fig. 11 Confusion matrix for dermoscopic images

The number of images in the resulting non-dermoscopic dataset is increased by carrying out data augmentation. Then, SMOTE was applied to resolve the problem of class imbalance in both dermoscopic and non dermoscopic images as melanoma images being the minority class impact the model's sensitivity. The data is then divided into training and validation sets and fed to a VGG-16 network, which received a training accuracy of 79.77% and a validation accuracy of 79%. The model was tested on both dermoscopic and non-dermoscopic images, giving sensitivity to melanoma at 91% and 87% respectively. Hence the model serves as a great starting point in terms of generalisability and scalability on both kinds of images.

As an extension to this work, this model can be further improved - reducing Type I and Type II errors and optimisation through better hyperparameter tuning such that it can scale on newer datasets taken from different distributions. The inclusion of newer datasets with images captured using different devices, varying resolutions and different levels of pre-processing can lead to a more robust, generalisable and fair model. Progress in such ventures can be very beneficial on the early diagnosis and medical assistance front, thereby reducing mortality rates.

VI. REFERENCES

[1] R. W. Jenkins and D. E. Fisher, "Treatment of Advanced Melanoma in 2020 and Beyond," *J. Invest. Dermatol.*, vol. 141, no. 1, pp. 23–31, 2021, doi: https://doi.org/10.1016/j.jid.2020.03.943.

[2] "Cancer, WHO." https://www.who.int/news-room/fact-sheets/detail/cancer.

[3] H. Sung *et al.*, "Global Cancer Statistics 2020: GLOBOCAN Estimates of Incidence and Mortality Worldwide for 36 Cancers in 185 Countries," *CA. Cancer J. Clin.*, vol. 71, no. 3, pp. 209–249, 2021, doi: 10.3322/caac.21660.

[4] "cancer-deaths-worldwide-by-major-type-2020." https://www.statista.com/statistics/288580/number-of-cancer-deaths-worldwide-by-type/.

[5] T. Petrie, R. Samatham, A. M. Witkowski, A. Esteva, and S. A. Leachman, "Melanoma Early Detection: Big Data, Bigger Picture," *J. Invest. Dermatol.*, vol. 139, no. 1, pp. 25–30, 2019, doi: https://doi.org/10.1016/j.jid.2018.06.187.

[6] E. Okur and M. Turkan, “A survey on automated melanoma detection,” *Eng. Appl. Artif. Intell.*, vol. 73, pp. 50–67, 2018, doi: https://doi.org/10.1016/j.engappai.2018.04.028.

[7] D. V. D. S. Abeysinghe and S. Sotheeswaran, “Novel computational approaches for border irregularity prediction to detect melanoma in skin lesions,” in *2020 International Research Conference on Smart Computing and Systems Engineering (SCSE)*, 2020, pp. 216–222, doi: 10.1109/SCSE49731.2020.9313042.

[8] E. Vocaturo, E. Zumpano, and P. Veltri, “Features for Melanoma Lesions Characterization in Computer Vision Systems,” in *2018 9th International Conference on Information, Intelligence, Systems and Applications (IISA)*, 2018, pp. 1–8, doi: 10.1109/IISA.2018.8633651.

[9] A. A. Marghoob and A. Scope, “The Complexity of Diagnosing Melanoma,” *J. Invest. Dermatol.*, vol. 129, no. 1, pp. 11–13, 2009, doi: https://doi.org/10.1038/jid.2008.388.

[10] D. S. Rigel, J. Russak, and R. Friedman, “The Evolution of Melanoma Diagnosis: 25 Years Beyond the ABCDs,” *CA. Cancer J. Clin.*, vol. 60, no. 5, pp. 301–316, 2010, doi: 10.3322/caac.20074.

[11] M. H. Jafari, E. Nasr-Esfahani, N. Karimi, S. M. R. Soroushmehr, S. Samavi, and K. Najarian, “Extraction of skin lesions from non-dermoscopic images for surgical excision of melanoma,” *Int. J. Comput. Assist. Radiol. Surg.*, vol. 12, no. 6, pp. 1021–1030, 2017, doi: 10.1007/s11548-017-1567-8.

[12] M. H. Jafari, S. Samavi, S. M. R. Soroushmehr, H. Mohaghegh, N. Karimi, and K. Najarian, “Set of descriptors for skin cancer diagnosis using non-dermoscopic color images,” in *2016 IEEE International Conference on Image Processing (ICIP)*, 2016, pp. 2638–2642, doi: 10.1109/ICIP.2016.7532837.

[13] S. Mustafa, A. B. Dauda, and M. Dauda, “Image processing and SVM classification for melanoma detection,” in *2017 International Conference on Computing Networking and Informatics (ICCNI)*, 2017, pp. 1–5, doi: 10.1109/ICCNI.2017.8123777.

[14] Z. Waheed, A. Waheed, M. Zafar, and F. Riaz, “An efficient machine learning approach for the detection of melanoma using dermoscopic images,” in *2017 International Conference on Communication, Computing and Digital Systems (C-CODE)*, 2017, pp. 316–319, doi: 10.1109/C-CODE.2017.7918949.

[15] D. Gautam, M. Ahmed, Y. K. Meena, and A. Ul Haq, “Machine learning–based diagnosis of melanoma using macro images,” *Int. j. numer. method. biomed. eng.*, vol. 34, no. 5, 2018, doi: 10.1002/cnm.2953.

[16] F. Xie, H. Fan, Y. Li, Z. Jiang, R. Meng, and A. Bovik, “Melanoma Classification on Dermoscopy Images Using a Neural Network Ensemble Model,” *IEEE Trans. Med. Imaging*, vol. 36, no. 3, pp. 849–858, 2017, doi: 10.1109/TMI.2016.2633551.

[17] E. Nasr-Esfahani *et al.*, “Melanoma detection by analysis of clinical images using convolutional neural network,” *Proc. Annu. Int. Conf. IEEE Eng. Med. Biol. Soc. EMBS*, vol. 2016-Octob, pp. 1373–1376, 2016, doi: 10.1109/EMBC.2016.7590963.

[18] X. Zhang, “Melanoma segmentation based on deep learning,” *Comput. Assist. Surg.*, vol. 22, no. 0, pp. 267–277, 2017, doi: 10.1080/24699322.2017.1389405.

[19] N. Nida, A. Irtaza, A. Javed, M. H. Yousaf, and M. T. Mahmood, “Melanoma lesion detection and segmentation using deep region based convolutional neural network and fuzzy C-means clustering,” *Int. J. Med. Inform.*, vol. 124, pp. 37–48, 2019, doi: https://doi.org/10.1016/j.ijmedinf.2019.01.005.

[20] S. R D and S. A, “Deep Learning Based Skin Lesion Segmentation and Classification of Melanoma Using Support Vector Machine (SVM).,” *Asian Pac. J. Cancer Prev.*, vol. 20, no. 5, pp. 1555–1561, May 2019, doi: 10.31557/APJCP.2019.20.5.1555.

[21] S. Vesal, N. Ravikumar, and A. Maier, “SkinNet: A Deep Learning Framework for Skin Lesion Segmentation,” in *2018 IEEE Nuclear Science Symposium and Medical Imaging Conference Proceedings (NSS/MIC)*, 2018, pp. 1–3, doi: 10.1109/NSSMIC.2018.8824732.

[22] Y. Ge, B. Li, Y. Zhao, E. Guan, and W. Yan, “Melanoma Segmentation and Classification in Clinical Images Using Deep Learning,” in *Proceedings of the 2018 10th International Conference on Machine Learning and Computing*, 2018, pp. 252–256, doi: 10.1145/3195106.3195164.

[23] M. H. Jafari, E. Nasr-Esfahani, N. Karimi, S. M. R. Soroushmehr, S. Samavi, and K. Najarian, “Extraction of Skin Lesions from Non-Dermoscopic Images Using Deep Learning,” pp. 10–11, 2016, doi: 10.1007/s11548-017-1567-8.

[24] J. Jaworek-Korjakowska, P. Kleczek, and M. Gorgon, “Melanoma thickness prediction based on convolutional neural network with VGG-19 model transfer learning,” *IEEE Comput. Soc. Conf. Comput. Vis. Pattern Recognit. Work.*, vol. 2019-June, pp. 2748–2756, 2019, doi: 10.1109/CVPRW.2019.00333.

[25] J. A. A. Salido and C. R. Ruiz, “Using Deep Learning to Detect Melanoma in Dermoscopy Images.”

[26] S. Hosseinzadeh Kassani and P. Hosseinzadeh Kassani, “A comparative study of deep learning architectures on melanoma detection,” *Tissue Cell*, vol. 58, no. April, pp. 76–83, 2019, doi: 10.1016/j.tice.2019.04.009.

[27] X. Dai, I. Spasić, B. Meyer, S. Chapman, and F. Andres, “Machine Learning on Mobile: An On-device Inference App for Skin Cancer Detection,” in *2019 Fourth International Conference on Fog and Mobile Edge Computing (FMEC)*, 2019, pp. 301–305, doi: 10.1109/FMEC.2019.8795362.

[28] T.-T. Do *et al.*, “Accessible Melanoma Detection Using Smartphones and Mobile Image Analysis,” *IEEE Trans. Multimed.*, vol. 20, no. 10, pp. 2849–2864, 2018, doi: 10.1109/TMM.2018.2814346.

[29] I. Giotis, N. Molders, S. Land, M. Biehl, M. F. Jonkman, and N. Petkov, “MED-NODE: A computer-assisted melanoma diagnosis system using non-dermoscopic images,” *Expert Syst. Appl.*, vol. 42, no. 19, pp. 6578–6585, 2015, doi: https://doi.org/10.1016/j.eswa.2015.04.034.

[30] “Dermnet Dataset.” http://www.dermnet.com/.

[31] T. Mendonça, P. M. Ferreira, J. S. Marques, A. R. S. Marcal, and J. Rozeira, “PH2 - A dermoscopic image database for research and benchmarking,” in *2013 35th Annual International Conference of the IEEE Engineering in Medicine and Biology Society (EMBC)*, 2013, pp. 5437–5440, doi: 10.1109/EMBC.2013.6610779.

[32] P. Tschandl, “The HAM10000 dataset, a large collection of multi-source dermatoscopic images of common pigmented skin lesions.” Harvard Dataverse, doi: doi:10.7910/DVN/DBW86T.

[33] J. Deng, W. Dong, R. Socher, L.-J. Li, K. Li, and L. Fei-Fei, “ImageNet: A large-scale hierarchical image database,” in *2009 IEEE Conference on Computer Vision and Pattern Recognition*, 2009, pp. 248–255, doi: 10.1109/CVPR.2009.5206848.